Spatial Distribution of the Mean Peak Age of Information in Wireless Networks

Praful D. Mankar, *Member, IEEE*, Mohamed A. Abd-Elmagid, *Student Member, IEEE*, and Harpreet S. Dhillon, *Senior Member, IEEE*

***Abstract*—This paper considers a large-scale wireless network consisting of source-destination (SD) pairs, where the sources send time-sensitive information, termed *status updates*, to their corresponding destinations in a time-slotted fashion. We employ Age of information (AoI) for quantifying the freshness of the status updates measured at the destination nodes under the preemptive and non-preemptive queueing disciplines with no storage facility. The non-preemptive queue drops the newly arriving updates until the update in service is successfully delivered, whereas the preemptive queue replaces the current update in service with the newly arriving update, if any. As the update delivery rate for a given link is a function of the interference field seen from the receiver, the temporal mean AoI can be treated as a random variable over space. Our goal in this paper is to characterize the spatial distribution of the mean AoI observed by the SD pairs by modeling them as a bipolar Poisson point process (PPP). Towards this objective, we first derive accurate bounds on the moments of success probability while efficiently capturing the interference-induced coupling in the activities of the SD pairs. Using this result, we then derive tight bounds on the moments as well as the spatial distribution of peak AoI (PAoI). Our numerical results verify our analytical findings and demonstrate the impact of various system design parameters on the mean PAoI.**

***Index Terms*—Age of information, bipolar Poisson point process, stochastic geometry, and wireless networks.**

I. Introduction

With the emergence of Internet of Things (IoT), wireless networks are expected to provide a reliable platform for enabling real-time monitoring and control applications. Many such applications, such as the ones related to air pollution or soil moisture monitoring, involve a large-scale deployment of IoT sensors, which would acquire updates about some underlying random processes and send them to the destination nodes (or monitoring stations). Naturally, accurate quantification of the freshness of status updates received at the destination nodes is essential in such applications. However, the traditional performance metrics of communication systems, like throughput and delay, are not suitable for this purpose since they do not account for the generation times of status updates. This has recently motivated the use of AoI to quantify the performance of communication systems dealing with the transmission of time-sensitive information [2]. This metric was first conceived in [3] for a simple queuing-theoretic model in which randomly generated update packets arrive at a source node according to a Poisson process, and then transmitted to a destination node using a first-come-first-served (FCFS) queuing discipline. In particular, AoI was defined in [3] as the time elapsed since the latest successfully received update packet at the destination node was generated at the source node. As evident from the definition, AoI is capable of quantifying how *fresh* the status updates are when they reach the destination node since it tracks the generation time of each update packet. As will be discussed next in detail, the analysis of AoI has mostly been limited to simple settings that ignore essential aspects of wireless networks, including temporal channel variations and random spatial distribution of nodes. This paper presents a novel spatiotemporal analysis of AoI in a wireless network by incorporating the effect of both the channel variations and the randomness in the wireless node locations to derive the spatial distribution of the temporal mean AoI.

P. D. Mankar is with SPCRC, IIIT Hyderabad, India (Email: praful.mankar@iiit.ac.in). M. A. Abd-Elmagid, and H. S. Dhillon are with Wireless@VT, Bradley Department of Electrical and Computer Engineering, Virginia Tech, Blacksburg, VA. Email: {maelaziz, hdhillon}@vt.edu. The support of the U.S. NSF (Grant CPS-1739642) is gratefully acknowledged. This paper will be presented in part at IEEE ICC 2021 [1].

A. Prior Art

For a point-to-point communication system, the authors of [3] characterized a closed-form expression for the average AoI. Subsequently, the authors of [4]–[11] characterized the average AoI or similar age-related metrics (e.g., PAoI [5], [8], [9] and Value of Information of Update [10]) for a variety of queuing disciplines. In addition, the authors of [12]–[16] presented the queuing theory-based analysis of the distribution of AoI. The above works provide foundational understanding of temporal variations of AoI from the perspective of queuing theory for a point-to-point communication system. Inspired by these works, the AoI or similar age-related metrics have been used to characterize the performance of real-time monitoring services in a variety of communication systems, including broadcast networks [17]–[19], multicast networks [20], [21], multi-hop networks [22], [23], multi-server information-update systems [24], IoT networks [25]–[30], cooperative device-to-device (D2D) communication networks [31], [32], unmanned aerial vehicle (UAV)-assisted networks [33], [34], ultra-reliable low-latency vehicular networks [35], and social networks [36]–[38]. All these studies mostly focus on minimizing the AoI with the following design objectives: 1) design of scheduling policies [17]–[19], [22], [30], 2) design of cooperative transmission policies [20]–[23], [31], [32], 3) design of the status update sampling policies [27]–[29], [36], and 4) trade-off with other performances metrics in heterogeneous traffic/networks scenarios [23]–[25], [29], [37]. However, given the underlying tools used, these works are not conducive to account for some

important aspects of wireless networks, such as interference, channel variations, path-loss, and random network topologies.

Over the last decade, the stochastic geometry has emerged as a powerful tool for the analysis of the large-scale random wireless networks while efficiently capturing the above propagation features. The interested readers, for examples, can refer to models and analyses presented in [39] for cellular networks, [40] for heterogeneous networks, and [41] for ad-hoc networks. While these works were initially focused on the space-time mean performance of network (such as *coverage probability*), a new performance metric is recently introduced, termed *meta distribution*, in [42] for characterizing the spatial variation in the temporal mean performance measured at the randomly located nodes. The meta distribution has become an instrumental tool for analyzing the spatial disparity in a variety of performance metrics (e.g., see [43]–[45]) and network settings (e.g., see [46], [47]). However, these stochastic geometry models lack to handle the traffic variations because of which they are mostly applicable to saturated networks. Therefore, it is important to develop a method/tool that is capable of handling in spatial randomness through interference and temporal variations due to traffic. But, in general, the spatiotemporal analysis is known to be hard, for the reasons discussed next.

The wireless links exhibit the space-time correlation through their interference-induced stochastic interactions [48]. This implies that the service rates of the wireless nodes are also correlated (in both space and time), which, as a result, generates coupling between the activities of their associated queues under random traffic patterns. The coupled queues cause difficulty in the spatiotemporal analysis of wireless networks. It is worth noting that the exact characterization of the correlated queues is unknown even in simple settings (refer to [49]). In the existing literature, there are broadly two approaches for the spatiotemproal analyses trying to capture the temporal traffic dynamics and spatial nodes variation to some extent. The first approach is focused on the development of iterative frameworks/algorithms specific to the performance metric of interest. In this approach, the queues are first decoupled by modeling the activity of each node independently using a spatial mean activity [50]–[54] (or, a spatial distribution of activity [45], [55]–[57]) and then the analytical framework is solved in an iterative manner until the spatial mean activity (or, the spatial distribution of activity) converge to its *fixed-point solution*. On the other hand, the second approach adopts to the approach used in queueing theory literature for obtaining the performance bounds on correlated queues (for example, see [49]). In this approach, the activities of nodes are decoupled by constructing *a dominant system* wherein the interfering nodes are considered to have the saturated queues [44], [58]–[60]. Because of their saturated queues, the activities of interfering nodes will increase. Thus, the observing node will overestimate the interference power, and hence, needless to say, its performance will be a bound. However, such a bound tends to get loosen when the traffic conditions are lighter, which is quite intuitive. In [58], a second degree of dominant system is presented wherein the interferers are assumed to operate under their corresponding dominant systems. Naturally, this second degree modifications will provide a better performance bound as it estimates the interference more accurately compared to the dominant system. In contrast, the coupling between their activities become insignificant when a massive number of nodes access the channel in a sporadic manner and thus it can be safely ignored in the analysis [61].

Nevertheless, there are only a handful of recent works focusing on the spatiotemproal analysis of AoI for wireless networks. For example, for a Poisson bipolar network, [57] derived the spatiotemporal average of AoI for an infinite-length FCFS queue, whereas [62] derived the spatiotemporal mean PAoI for a unit-length last-come-first-served (LCFS) queue with replacement. The authors first obtained a fixed point solution to the meta distribution in an iterative manner and then applied it to determine the spatiotemporal mean AoI. The authors of [62] also investigated a locally adaptive scheduling policy that minimizes the mean AoI. Further, [60] derived the upper and lower bounds on the cumulative distribution function (CDF) of the temporal mean AoI for a Poisson bipolar network using the construction of dominant system. On the other hand, the spatiotemporal analysis of PAoI for uplink IoT networks is presented in [45], [51], [63] by modeling the locations of BSs and IoT devices using independent PPPs. The authors of [45] derived the mean PAoI for time-triggered (TT) and event-triggered (ET) traffic. The authors employed an iterative framework wherein quantized meta distribution and spatial average activities of devices with different classes (properly constructed based on TT and ET traffic) are determined together. Further, [51] derived the mean PAoI for the prioritized multi-stream traffic (PMT) by iteratively solving the queueing theoretic framework (developed for PMT) and priority class-wise successful transmission probabilities together. The authors of [63] derived the spatial distribution of the temporal mean PAoI while assuming the IoT devices sample their updates using *generate-at-will* policy (see [2]). Besides, it is worth noting that the delay analyses presented in [52], [53], [55], [56] can be extended to analyze the PAoI under FCFS queuing discipline.

B. Contributions

This paper presents a stochastic geometry-based analysis of PAoI for a large-scale wireless network, wherein the sources transmit time-sensitive status updates to their corresponding destinations. In particular, we derive the spatial distribution of temporal mean PAoI while assuming that the locations of SD pairs follow a homogeneous bipolar PPP. In order to overcome the challenge of interference-induced coupling across queues associated with different SD pairs, we propose a tractable two-step analytical approach which relies on a careful construction of *dominant systems*. The proposed framework efficiently captures the stochastic interaction in both space (through interference) and time (through random transmission activities). Our approach provides a much tighter lower bound on the spatial moments of the conditional (location-dependent) successful transmission probability compared to the existing stochastic geometry-based analyses, e.g., [44], which mainly rely on the assumption of having saturated queues at the interfering nodes.

The above construction of dominant system allows to model the upper bound of service times of the update transmissions using geometric distribution. Further, assuming the Bernoulli arrival of status update, we model status update transmissions using Geo/Geo/1 queue with no storage facility under pre-emptive and non-preemptive disciplines. For this setup, we present the spatiotemproal analysis of the PAoI. In particular, we derive tight upper bounds on the spatial moments of the temporal mean PAoI for the above queue disciplines. The contributions of this paper are briefly summarized as below.

1) This paper presents a novel analytical framework to determine tight lower bounds on the moments of the conditional success probability while efficiently capturing the interference-induced coupling in the activities of SD pairs.
2) We derive the temporal mean of PAoI under both pre-emptive and non-preemptive queueing disciplines for a given success probability of transmission.
3) Next, using the lower bounds on the moments of the conditional success probability, we derive tight upper bounds on the spatial moments of the temporal mean PAoI for both queuing disciplines.
4) Using the beta approximation for the distribution of conditional success probability [42], we also characterize the spatial distribution of temporal mean PAoI.
5) Next, we validate the accuracy of the proposed analytical framework for AoI analysis through extensive simulations. Finally, our numerical results reveal the impact of key design parameters, such as the medium access probability, update arrival rate, and signal-to-interference (SIR) threshold, on the spatial mean and standard deviation of the temporal mean PAoI observed under the aforementioned queuing disciplines.

II. System Model

We model SD pairs using a static network wherein the locations of sources are distributed according to a PPP Φ with density λ_{sd} and their corresponding destinations are located at fixed distance R from them in uniformly random directions. The SIR measured at the destination at $\mathbf{z}$ in the k-th transmission slot is

$$\mathtt{SIR}_{\mathbf{z},k} = \frac{h^k_{\mathbf{z}} R_o^{-\alpha}}{\sum_{\mathbf{x}\in\Phi} h^k_{\mathbf{x},\mathbf{z}} \|\mathbf{x}-\mathbf{z}\|^{-\alpha} \mathbb{1}(\mathbf{x}\in\Phi_k)}, \tag{1}$$

where Φ_k is the set of sources with active transmission during the k-th transmission slot, and $\mathbb{1}(\mathbf{x}\in\Phi_k)$ is 1 if $\mathbf{x}\in\Phi_k$, otherwise 0. α is the path-loss exponent, and $h^k_{\mathbf{z}}$ and $h^k_{\mathbf{x},\mathbf{z}}$ are the channel gains for the link from desired source and the link from the source at $\mathbf{x}$ to the destination at $\mathbf{z}$, respectively, in transmission slot k. We assume quasi-static Rayleigh fading model, which implies $h^k_{\mathbf{x},\mathbf{z}} \sim \exp(1)$ independently across both $\mathbf{x}\in\Phi$ and $k\in\mathbb{N}$.

Since the point process of SD pairs is assumed to be stationary, the distribution of SIR observed by the different devices across a large-scale static realization of network is equivalent to the distribution of SIR measured at a fixed point across multiple realizations. This can be formalized using *Palm distribution*, which is the conditional distribution of the point process given that the typical point is present at a fixed location. Further, by the virtue of Slivnyak's theorem, we know that the Palm distribution for PPP is the same as the original distribution of PPP. Please refer to [64] for more details. Therefore, we place the typical SD pair link such that its destination and source are at the origin o and $\mathbf{x}_o \equiv [R, 0]$, respectively. Fig. 1 presents a representative realization of the bipolar Poisson network with the typical link at $(o, \mathbf{x}_o)$. As the analysis is focused on this typical link, we drop the subscript $\mathbf{z}$ from $\mathtt{SIR}_{\mathbf{z},k}$ and $h^k_{\mathbf{x},\mathbf{z}}$ here onwards.

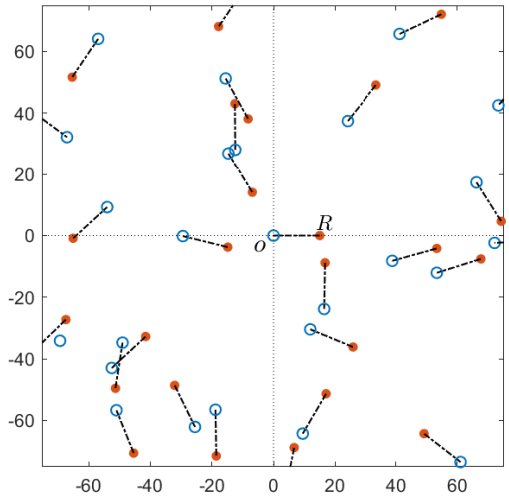

Figure 1. A typical realization of the bipolar Poisson network for $\lambda_{\text{sd}} = 10^{-3}$ links/m^2 and $R = 15$ m. Orange dots and blue circles represent the locations of sources and destinations, respectively.

A. Conditional Success Probability

The transmission is considered to be successful when the received SIR is greater than a threshold β. From (1), it is clear that the successful transmission probability measured at the typical destination placed at o depends on the PPP Φ of the interfering sources and is given by

$$\begin{aligned}\mu_\Phi &= \mathbb{P}[\mathtt{SIR}_k > \beta|\Phi] \\ &= \mathbb{P}\left[h^k_{\mathbf{x}_o} > \beta R^\alpha \sum\nolimits_{\mathbf{x}\in\Phi} h^k_{\mathbf{x}} \|\mathbf{x}\|^{-\alpha} \mathbf{1}(\mathbf{x}\in\Phi_k)\big|\Phi\right], \\ &= \mathbb{E}\left[\exp\left(-\beta R^\alpha \sum\nolimits_{\mathbf{x}\in\Phi} h^k_{\mathbf{x}} \|\mathbf{x}\|^{-\alpha} \mathbf{1}(\mathbf{x}\in\Phi_k)\right)|\Phi\right], \\ &= \prod_{\mathbf{x}\in\Phi}\left[\frac{p_{\mathbf{x}}}{1+\beta R^\alpha \|\mathbf{x}\|^{-\alpha}} + (1-p_{\mathbf{x}})\right], \end{aligned} \tag{2}$$

where $p_{\mathbf{x}}$ represents the probability that the source at $\mathbf{x}\in\Phi$ is active. Note that the time-average activity $p_{\mathbf{x}}$ for source at $\mathbf{x}$ is used in (2). This implies that the typical destination observes the activities of interfering sources as a time-homogeneous process at any given transmission slot. This assumption will help to develop a new framework for an accurate spatiotemporal analysis, as will be evident shortly. The conditional success probability μ_Φ will be useful to determine the packet delivery rate over the typical link for a given Φ. Thus, the knowledge of the meta distribution, defined below, is crucial to characterize the queue performance for the typical link.

Definition 1 (Meta Distribution)**.** *The meta distribution of* SIR

is defined in [42] as

$$\mathrm{D}(\beta, x) = \mathbb{P}[\mathbb{P}[\mathtt{SIR}_k > \beta|\Phi] > x] = \mathbb{P}[\mu_\Phi > x], \quad (3)$$

where μ_Φ, given in (2), is the conditional success probability measured at the typical destination for a given Φ.

B. Traffic Model and AoI Metric

We consider that the source at $\mathbf{x} \in \Phi$ transmits updates to the corresponding destination regarding its associated physical random process $H_{\mathbf{x}}(t)$. Each source (independently of others) is assumed to sample its associated physical random process at the beginning of each transmission slot according to a Bernoulli process with parameter λ_{a}. This assumption of a fixed parameter Bernoulli process for modeling the update arrivals can be seen is a necessary approximation of a scenario where the sources may observe different physical random processes. However, one can relax the fixed arrival rate assumption with a few but straightforward modifications to the analysis presented in this paper.

The transmission is considered to be successful if SIR received at the destination is above threshold β. Thus, the source is assumed to keep transmitting a status update until it receives the successful transmission acknowledgement from the destination on a separate feedback channel, which is assumed to be error free. The successful delivery of an update takes a random number of transmissions depending on the channel conditions that further depend on numerous factors, such as fading coefficients, received interference power, and network congestion. Links that are in close proximity of each other may experience arbitrarily small update delivery rate because of severe interference, especially when update arrival rate is high. Therefore, to alleviate the impact of severe interference in such cases, we assume that each source attempts transmission with probability ξ independently of the other sources in a given time slot. Also note that the probability of the attempted transmission being successful in a given time slot is the conditional success probability μ_Φ because of the assumption of independent fading. Therefore, the number of slots needed for delivering an update at the typical destination can be modeled using the geometric distribution with parameter $\xi\mu_\Phi$ for a given Φ.

Let t_k and t'_k be the instances of the arrival (or, sampling) and reception of the k-th update at the source and destination, respectively. Given time slot n, let $D_n = \max\{k|t'_k \leq n\}$ be the slot index of the most recent update received at the destination and A_n be the slot index of the arrival (at source) of the most recent update received at destination (i.e., at D_n). The AoI of the status update at n-th slot is

$$\Delta(n) = \begin{cases} \Delta(n-1)+1, & \text{if transmission fails} \\ \Delta(n-1)+1-A_n, & \text{otherwise.} \end{cases} \quad (3)$$

The AoI $\Delta(n)$ increases in a staircase fashion with time and drops upon reception of a new update at the destination to the total number of slots experienced by this new update in the system. Note that the minimum possible AoI is one because we assume arrival and delivery of an update to occur at the beginning and the end of the transmission slots, respectively. Given this background, we are now ready to define PAoI, which will be studied in detail in this paper.

Definition 2 (PAoI)**.** *The PAoI is defined in [5] as the value of AoI process $\Delta(n)$ measured immediately before the reception of the k-th update and is given by*

$$A_k = T_{k-1} + Y_k. \quad (4)$$

where $T_k = t'_k - t_k$ is the time spent by the k-th update in the system and $Y_k = t'_k - t'_{k-1}$ is the time elapsed between the receptions of the $(k-1)$-th and k-th updates.

As evident from the above discussion, the mean PAoI measured at the typical destination depends on the conditional success probability μ_Φ and hence the conditional mean PAoI is a random variable. Therefore, our goal is to determine the distribution of the conditional mean PAoI of the SD pairs distributed across the network. In the following, we define the distribution of conditional mean PAoI.

Definition 3 (Conditional mean PAoI)**.** *For a given Φ, the conditional (temporal) mean PAoI measured at the typical destination is defined as*

$$\bar{A}(\beta; \Phi) = \mathbb{E}[A_k|\beta; \Phi], \quad (5)$$

and the complementary CDF of $\bar{A}(\beta; \Phi)$ is defined as

$$\bar{F}(x; \beta) = \mathbb{P}[\bar{A}(\beta; \Phi) > x], \quad (6)$$

where β is the SIR threshold.

C. Queue Disciplines

As discussed in Section I-A, the construction of the dominant system allows to decouple the activity of typical link with the activities of other links. Thus, for a given Φ, the service rate of the typical link becomes time-invariant (but a lower bound) in the dominant system. This implies that the service process can be modeled using the geometric distribution for analyzing the conditional performance bounds of the queue associated with the typical link. Therefore, with the above discussed Bernoulli sampling, we can model the status update transmissions over the typical link using Geo/Geo/1 with arrival and service rates equal to λ_{a} and $\xi\mu_\Phi$, respectively, for a given Φ. In particular, we consider Geo/Geo/1 queue with no storage facility (i.e., zero buffer) under preemptive and non-preemptive disciplines. In preemptive case, the older update in service (or, retransmission) is discarded upon the arrival of a new update. However, in non-preemptive case, the newly arriving updates are discarded until the one in service is successfully delivered. The disadvantage of non-preemptive discipline is that if the server takes a long time to transmit the packet (because of failed transmission attempts), the update in the server gets stale, which impacts AoI at the destination. On the contrary, under the preemptive discipline, the source always ends up transmitting the most recent update available at the successful transmissions. Thus, this discipline is optimal from the perspective of minimizing AoI. Nonetheless, the mean AoIs under both disciplines are almost the same for the sources experiencing high service rates, as will be evident shortly. That said, the analysis of non-preemptive discipline is still important because it acts as the precursor for the more complicated analysis of preemptive discipline.

Here onward, we will append subscripts P and NP to $\bar{A}(\beta;\Phi)$ to denote the conditional mean PAoI under the preemptive and non-preemptive queueing disciplines, respectively. We first present the analysis of $\bar{A}_{\mathrm{NP}}(\beta;\Phi)$ in Section III. Next, we extend the analysis to obtain $\bar{A}_{\mathrm{P}}(\beta;\Phi)$ in Section IV using the analytical framework developed in Section III.

III. AoI under non-preemptive Geo/Geo/1 queue

In non-preemptive discipline, each source transmits the updates on the first arrival basis without buffering them. As a result, the updates arriving during the ongoing transmission (i.e., busy server) are dropped. The sample path of the AoI process for this discipline is illustrated in Fig. 2. The red

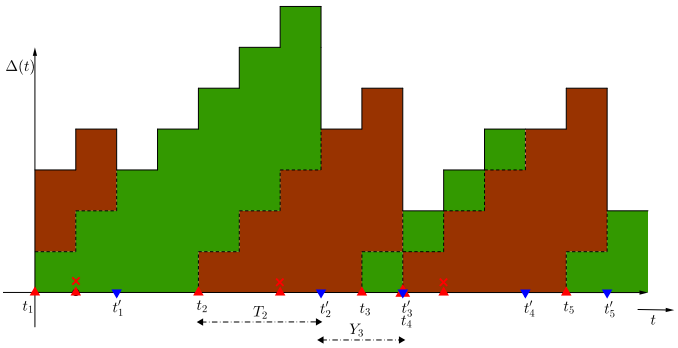

Figure 2. Sample path of the AoI $\Delta(t)$ under the non-preemptive discipline.

upward and blue downward arrow marks indicate the arrival and reception of updates at the source and destination, respectively. The red cross marks indicate the instances of dropped updates which arrive while the server is busy. We first derive the conditional mean PAoI in the following subsection. In the subsequent subsections, we will develop an approach to derive the distribution of the conditional mean PAoI using stochastic geometry.

A. Conditional Mean PAoI

As discussed before, the update delivery rate is governed by the product of the medium access probability ξ and the conditional success probability μ_Φ. Thus, for a given Φ, the probability mass function (pmf) of number of time slots required for a successful transmission is

$$\mathbb{P}[T_k = n] = \xi\mu_\Phi(1-\xi\mu_\Phi)^{n-1}, \quad \text{for } n = 1, 2, \ldots \tag{7}$$

Thus, we can obtain $\mathbb{E}[T_k] = \xi^{-1}\mu_\Phi^{-1}$. Since we assumed zero length buffer queue, the next transmission is possible only for the update arriving after the successful reception of the ongoing update. Therefore, the time between the successful reception of $(k-1)$-th and k-th updates is

$$Y_k = V_k + T_k, \quad \text{such that } Y_k \geq 1,$$

where V_k is the number of slots required for the k-th update to arrive after the successful delivery of the $(k-1)$-th update. It is worth noting that the inequality $Y_k \geq 1$ follows from the assumption of the transmission of an update begins in the same slot in which it arrives. Also, the inequality $V_k \geq 0$ (necessary to hold $Y_k \geq 1$ since $T_k \geq 1$) is quite evident as the next update can arrive at the beginning of next transmission slot after successful reception. Therefore, using the Bernoulli arrival of status updates, we can obtain pmf of V_k as below

$$\mathbb{P}[V_k = n] = \lambda_{\mathrm{a}}(1-\lambda_{\mathrm{a}})^n, \quad \text{for } n = 0, 1, 2, \ldots \tag{8}$$

Using the above pmf, we can obtain $\mathbb{E}[V_k] = \mathcal{Z}_{\mathrm{a}} = \frac{1}{\lambda_{\mathrm{a}}} - 1$. Now, from (4), the conditional mean PAoI for given Φ becomes

$$\bar{A}_{\mathrm{NP}}(\beta;\Phi) = \mathcal{Z}_{\mathrm{a}} + \frac{2}{\mu_\Phi\xi}. \tag{9}$$

Using (9) and the distribution of μ_Φ, we can directly determine the distribution of $\bar{A}_{\mathrm{NP}}(\beta;\Phi)$. However, from (2), it can be seen that the knowledge of probability $p_{\mathbf{x}}$ of the interfering source at $\mathbf{x} \in \Phi$ being active is required to determine the distribution of μ_Φ. For this, we first determine the activity of the typical source for a given μ_Φ in the following subsection which will later be used to define the activities of interfering sources in order to characterize the distribution of μ_Φ.

B. Conditional Activity

As each source is assumed to transmit independently in a given time slot with probability ξ, the conditional probability of the typical source having an active transmission becomes

$$\zeta_o = \xi\pi_1, \tag{10}$$

where π_1 is the conditional steady state probability that the source has an update to transmit. Thus, ζ_o depends on the probability $p_{\mathbf{x}}$ of the interfering source at $\mathbf{x} \in \Phi$ being active through the conditional success probability μ_Φ (see (2)). The

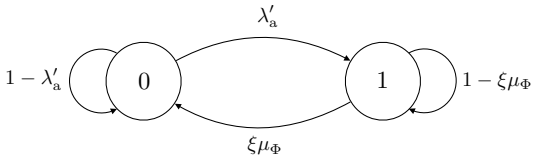

Figure 3. State Diagram of the Geo/Geo/1 queue. States 0 and 1 respectively signify idle and busy states of the typical source.

steady state distribution of a queue is characterized by its arrival and departure processes. In our case, both the arrivals and departures of the updates of $H(t)$ follow geometric distributions with parameters $\lambda'_{\mathrm{a}} = \mathcal{Z}_{\mathrm{a}}^{-1}$ and $\xi\mu_\Phi$, respectively. Fig. 3 shows the state diagram for the Geo/Geo/1 queue. Let π_0 and π_1 be the steady state probabilities of states 0 and 1, respectively. Thus, we have

$$\pi_0 = \frac{\xi\mu_\Phi}{\lambda'_{\mathrm{a}} + \xi\mu_\Phi} \quad \text{and} \quad \pi_1 = \frac{\lambda'_{\mathrm{a}}}{\lambda'_{\mathrm{a}} + \xi\mu_\Phi}. \tag{11}$$

C. Meta Distribution

From the above it is clear that the mean PAoI jointly depends on the PPP Φ of the interfering sources and their activities $p_{\mathbf{x}}$ through the conditional success probability μ_Φ. Hence, the knowledge of the exact distribution of μ_Φ, i.e., $\mathbb{P}[\mu_\Phi \leq x]$, is essential for characterizing the spatial distribution of the mean PAoI. However, it is very challenging to capture the temporal correlation among the activities of the sources in the analysis. Therefore, we derive the moments and approximate distribution of μ_Φ in the following lemma while

assuming the activities $p_{\mathbf{x}}$ to be independent and identically distributed (i.i.d.).

Lemma 1. *The b-th moment of the conditional success probability μ_Φ is*

$$M_b = \exp\left(-\pi\lambda_{sd}\beta^\delta R^2\hat{\delta}C_{\zeta_o}(b)\right), \tag{12}$$

where $\delta = \frac{2}{\alpha}$, $\hat{\delta} = \Gamma(1+\delta)\Gamma(1-\delta)$ and

$$C_{\zeta_o}(b) = \sum_{m=1}^{\infty}\binom{b}{m}\binom{\delta-1}{m-1}\bar{p}_m,$$

and $\bar{p}_m$ is the m-th moment of the activity probability. The meta distribution can be approximated with the beta distribution as

$$\mathrm{D}(\beta, x) \approx 1 - B_x(\kappa_1, \kappa_2), \tag{13}$$

where $B_x(\cdot,\cdot)$ is the regularized incomplete beta function and

$$\kappa_1 = \frac{M_1\kappa_2}{1-M_1} \quad \textit{and} \quad \kappa_2 = \frac{(M_1-M_2)(1-M_1)}{M_2-M_1^2}. \tag{14}$$

Proof. Please refer to Appendix A for the proof of moments of μ_Φ. □

The calculation of the $\bar{p}_m$ will be presented in the next subsection. It must be noted that the distribution of the conditional success probability μ_Φ is approximated using the beta distribution by equating the first two moments, similar to [42]. Now, we present an approach for accurate characterization of μ_Φ in the following subsection.

D. A New Approach for Spatiotemporal Analysis

As discussed in Section III-B, the activity of the typical source depends on its successful transmission probability which further depends on the activities of the other sources in Φ through interference (refer to (2)). Besides, the transmission of the typical source causes strong interference to its neighbouring sources which in turn affects their activities. Hence, the successful transmission probabilities of the typical source and its neighbouring sources are correlated through interference which introduces coupling between the operations of their associated queues. As discussed in Section I-A, the spatiotemproal analysis under the correlated queues is complex. Hence, we adopt to the approach of constructing a dominant system for analyzing the performance bound on conditional success probability and thereby on the conditional mean PAoI.

On the similar lines of [58], we present a novel two-steps analytical framework to enable an accurate success probability analysis using stochastic geometry while accounting for the temporal correlation in the queues associated with the SD pairs.

• *Step 1 (*Dominant System*):* For the dominant system, the interfering sources having no updates to transmit are assumed to transmit dummy packets with probability ξ. As a result, the success probability measured at the typical destination is a lower bound to that in the original system. The b-th moment and approximate distribution of μ_Φ for the dominant system can be evaluated using Lemma 1 by setting $\bar{p}_m = \xi^m$. Using (10), we can obtain the distribution of the activity of the typical source in the dominant system as

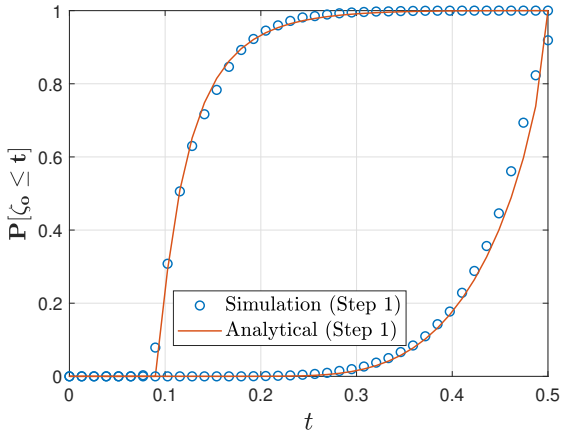

Figure 4. CDF of the activity in the dominant system for $\lambda_{\mathrm{a}} = 0.1$, $\xi = 0.5$, $\beta = 2$, $\alpha = 4$, $R = 10$, and $\lambda_{\mathrm{sd}} = \{10^{-3}, 10^{-4}\}$.

$$\begin{aligned}\mathbb{P}[\zeta_o \le t] &= \mathbb{P}\left[\lambda'_{\mathrm{a}}\left(\frac{1}{t}-\frac{1}{\xi}\right) \le \mu_\Phi\right], \\ &\approx 1 - B_{\lambda'_{\mathrm{a}}\left(\frac{1}{t}-\frac{1}{\xi}\right)}(\kappa_1,\kappa_2),\end{aligned} \tag{15}$$

for $0 < t \le \xi$, where κ_1 and κ_2 are evaluated using (14) with $\bar{p}_m = \xi^m$. It is quite evident that the activity ζ_o is less than ξ which is also consistent with the assumption of setting $p_{\mathbf{x}} = \xi$ for $\forall \mathbf{x} \in \Phi$ to define the dominant system. Fig. 4 illustrates the accuracy of the above approximate distribution of the activity of the typical source under the dominant system. Using (15), the m-th moment of the activity of the typical source in this dominant system can be evaluated as

$$\begin{aligned}\bar{p}_m^{\mathrm{D}} &= m\int_0^{\xi} t^{m-1}\mathbb{P}[\zeta_o > t]\mathrm{d}t, \\ &= m\int_0^{\xi} t^{m-1}B_{\lambda'_{\mathrm{a}}\left(\frac{1}{t}-\frac{1}{\xi}\right)}(\kappa_1,\kappa_2)\mathrm{d}t,\end{aligned} \tag{16}$$

where κ_1 and κ_2 are evaluated using (14) with $\bar{p}_m = \xi^m$.

• *Step 2 (Second-Degree of System Modifications):* Inspired by [58], we construct a second-degree system in which each interfering source is assumed to operate in its dominant system described in Step 1 (i.e., the interference field seen by a given interfering source is constructed based on Step 1). The typical SD link is now assumed to operate under these interfering courses. Naturally, the activities of the interfering sources will be higher in this modified system compared to those in the original system. As a result, the typical SD link will experience increased interference, and hence its conditional success probability will be a lower bound to that in the original system. It is easy to see that activities of the sources (in their dominant systems) are identically but not independently distributed. However, as is standard in similar stochastic geometry-based investigations, we will assume them to be independent to make the analysis tractable. In other words, we model the activities of the interfering sources in this modified system independently using the activity distribution presented in (15) for the typical SD link in its dominant system. As demonstrated in Section V, this assumption does not impact the accuracy of our results. Hence, similar to Step 1, the b-th moment and the approximate distribution of μ_Φ for

this second-degree modified system can be determined using Lemma 1 by setting $\bar{p}_m = \bar{p}_m^{\mathrm{D}}$.

E. Moments and Distribution of $\bar{A}_{\mathrm{NP}}(\beta;\Phi)$

Here, we derive the bounds on the moments and distribution of $\bar{A}_{\mathrm{NP}}(\beta;\Phi)$ using the two-step analysis of conditional success probability presented in Sections III-C and III-D.

Theorem 1. *The upper bound of the b-th moment of the conditional mean PAoI for non-preemptive queuing discipline with no storage is* $P_b =$

$$\sum_{n=0}^{b}\binom{b}{n}\mathcal{Z}_a^{b-n}2^n\xi^{-n}\exp\left(-\pi\lambda_{sd}\beta^{\delta}R^2\hat{\delta}C_{\zeta_o}(-n)\right), \quad (17)$$

$$\text{where} \quad C_{\zeta_o}(-n)=\sum_{m=1}^{\infty}\binom{-n}{m}\binom{\delta-1}{m-1}\bar{p}_m^{\mathrm{D}},$$

and $\bar{p}_m^{\mathrm{D}}$ is given in (16).

Proof. Using (9), the b-th moment of the conditional mean PAoI can be determined as

$$P_b=\mathbb{E}_{\Phi}\left[(2(\xi\mu_{\Phi})^{-1}+\mathcal{Z}_{\mathrm{a}})^b\right],$$
$$\overset{(a)}{=}\sum_{n=0}^{b}\binom{b}{n}\mathcal{Z}_{\mathrm{a}}^{b-n}2^n\xi^{-n}M_{-n} \quad (18)$$

where (a) follows using the binomial expansion and $\mathbb{E}[\mu_{\Phi}^{-n}]=M_{-n}$. According to the Step 2 discussed in Subsection III-D, M_{-n} can be obtained using Lemma 1 by setting $\bar{p}_m=\bar{p}_m^{\mathrm{D}}$. Recall that the two-step analysis provides a lower bound on the success probability μ_{Φ} because of overestimating the activities of the interfering sources. Therefore, the b-th moment of $\bar{A}_1(\beta;\Phi)$ given in (17) is indeed an upper bound since $\bar{A}_1(\beta;\Phi)$ is inversely proportional to μ_{Φ}. □

In the following corollary, we present the simplified expressions for the evaluation of the first two moments of $\bar{A}_1(\beta;\Phi)$.

Corollary 1. *The upper bound of the first two moments of the conditional mean PAoI for non-preemptive queuing discipline with no storage are*

$$P_1=\mathcal{Z}_a+2\xi^{-1}M_{-1} \quad (19)$$
$$P_2=\mathcal{Z}_a^2+4\mathcal{Z}_a\xi^{-1}M_{-1}+4\xi^{-2}M_{-2} \quad (20)$$

and the upper bound of its variance is

$$\mathtt{Var}=4\xi^{-2}\left(M_{-2}-M_{-1}^2\right), \quad (21)$$

where $M_l=\exp\left(-\pi\lambda_{sd}\beta^{\delta}R^2\hat{\delta}C_{\zeta_o}(l)\right)$, *distribution of ζ_o is given in* (15), *and*

$$C_{\zeta_o}(-1)=-\mathbb{E}\left[\zeta_o(1-\zeta_o)^{\delta-1}\right], \quad (22)$$
$$\text{and } C_{\zeta_o}(-2)=(\delta-1)\mathbb{E}\left[\zeta_o(1-\zeta_o)^{\delta-2}\right]$$
$$-(\delta+1)\mathbb{E}\left[\zeta_o(1-\zeta_o)^{\delta-1}\right]. \quad (23)$$

Proof. Please refer to Appendix B for the proof. □

Remark 1. *For the mean PAoI given in* (19), *the first term captures the impact of the update arrival rate λ_a whereas the second term depends on the inverse mean of the conditional success probability, which captures the impact of the wireless link parameters such as the link distance R, network density λ_{sd}, and path-loss exponent α. Furthermore, it is worth noting that the variance of the temporal mean AoI is independent of the arrival rate and entirely depends on the link quality parameters. This is because the arrival rate is assumed to be the same for all SD links and it corresponds to the additive term in conditional mean PAoI given in* (9).

Now, using the beta approximation of the conditional success probability presented in Lemma 1, we determine the distribution of $\bar{A}_{\mathrm{NP}}(\beta;\Phi)$ in the following corollary.

Corollary 2. *Under the beta approximation, the* CDF *of the conditional mean PAoI for non-preemptive queueing discipline is*

$$F(x;\beta)=1-B_{2\xi^{-1}(x-\mathcal{Z}_{\mathrm{a}})^{-1}}(\kappa_1,\kappa_2), \quad (24)$$

where κ_1 and κ_2 are obtain using Lemma 1 by setting $\bar{p}_m=\bar{p}_m^{\mathrm{D}}$.

Proof. Using (9) and the beta approximation of the distribution of μ_{Φ} given in Lemma 1, we can determine the distribution of $\bar{A}_1(\beta;\Phi)$ as

$$\mathbb{P}[\bar{A}_{\mathrm{NP}}(\beta;\Phi)\le x]=\mathbb{P}\left[\mu_{\Phi}\ge 2\xi^{-1}(x-\mathcal{Z}_{\mathrm{a}})^{-1}\right],$$
$$=\mathrm{D}(2\xi^{-1}(x-\mathcal{Z}_{\mathrm{a}})^{-1}).$$

Further, using the beta approximation for the distribution of μ_{Φ} (given in Lemma 1), we obtain (24). The parameters κ_1 and κ_2 need to be determined for $\bar{p}_m=\bar{p}_m^{\mathrm{D}}$ (refer to Section III-D). □

IV. AoI under preemptive Geo/Geo/1 queue

In preemptive discipline, each source transmits the most recent update available at the source in a given transmission slot. As a result, this queueing discipline helps to reduce the AoI which is clearly significant when the update arrival rate is high while the delivery rate is low. This discipline is, in fact, optimal from the perspective of minimizing AoI at the destination as the source always ends up transmitting its most recent update arrival. A representative sample path of the AoI process under the preemptive queue discipline is presented in Fig. 5. The red upward and blue downward arrow marks indicate the time instants of update arrivals at the source and deliveries at the destination, respectively. The red plus sign marks indicate the instances of replacing the older update with a newly arrived update and $t_{k,n}$ highlighted in red indicates the n-th replacement of the k-th update.

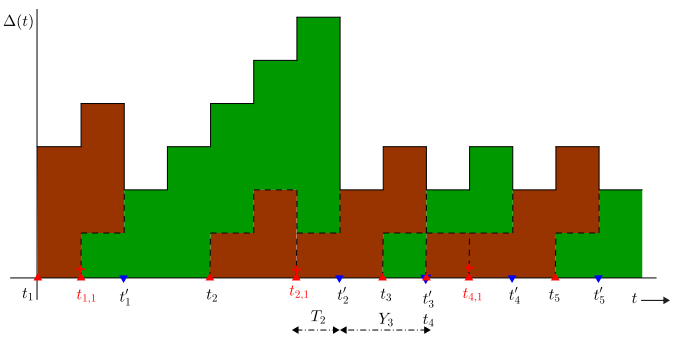

Figure 5. Sample path of the AoI $\Delta(t)$ under the preemptive queue discipline.

A. Conditional Mean PAoI

In this subsection, we derive the conditional mean PAoI for the typical destination for a given Φ. For this, the primary step is to obtain the means of the inter-departure time Y_k and service time T_k for a given conditional success probability μ_Φ (measured at the typical destination). While it is quite straightforward to determine the mean of Y_k, the derivation of the mean of T_k needs careful consideration of the successive replacement of updates until the next successful transmission occurs.

Mean of Y_k: Recall that the expected time for a new arrival is $\mathcal{Z}_\mathrm{a} = \frac{1}{\lambda_\mathrm{a}} - 1$. Also, recall that the update delivery rate is $\xi\mu_\Phi$ which follows from the fact that both the successful transmission and the medium access are independent events across transmission slots. Thus, since the transmission starts from the new arrival of the update after the successful departure, the mean time between two departures simply becomes

$$\mathbb{E}[Y_k] = \mathcal{Z}_\mathrm{a} + \frac{1}{\xi\mu_\Phi}. \tag{25}$$

Mean and Distribution of Delivery Times: The delivery times restart after every new update arrival before epochs of successful delivery. Let $\hat{T}_k$ be the delivery times of the latest

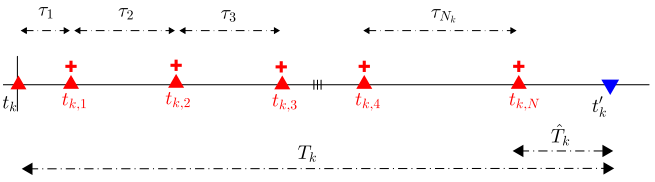

Figure 6. Illustration of the process $\hat{T}_k$ under preemption.

update under preemptive queueing disciple. Fig. 6 illustrates the typical realization of random process $\hat{T}_k$. The number of slots required to deliver the latest update, i.e. $\hat{T}_k$, is given by

$$\hat{T}_k = T_k - X_{N_k},$$

where $X_{N_k} = \sum_{i=1}^{N_k} \tau_i$, and N_k is the number of new update arrivals occurring between the arrival of the k-th update (right after $(k-1)$-th successful transmission) and the k-th successful transmission, and τ_n is the number of slots between the arrivals of two successive updates.

Lemma 2. *For a zero buffer queue with preemption, the* `pmf` *of number of slots required to deliver the latest update follows a geometric distribution as given below*

$$\mathbb{P}[\hat{T}_k = m] = q_\mathrm{s}(1-q_\mathrm{s})^{m-1}, \qquad \text{for } m = 1, 2, \ldots \tag{26}$$

where $q_\mathrm{s} = \xi\mu_\Phi + \lambda_a(1-\xi\mu_\Phi)$.

Proof. Please refer to the Appendix C for the proof. □

Now, the following theorem presents the moment generating function (`mgf`) of the conditional PAoI A_k for a given Φ.

Theorem 2. *For a zero buffer queue with preemption, the* `mgf` *of the conditional PAoI is* $\mathcal{M}_{\mathrm{P},A_k}(t) =$

$$\frac{\lambda_\mathrm{a}\xi\mu_\Phi q_\mathrm{s} e^{2t}}{(1-(1-\lambda_\mathrm{a})e^t)(1-(1-\xi\mu_\Phi)e^t)(1-(1-q_\mathrm{s})e^t)}, \tag{27}$$

and the mean of the conditional PAoI is

$$\bar{A}_\mathrm{P}(\beta;\Phi) = \mathcal{Z}_a + \frac{1}{\xi\mu_\Phi} + \frac{1}{q_\mathrm{s}}, \tag{28}$$

where $q_\mathrm{s} = \xi\mu_\Phi + \lambda_a(1-\xi\mu_\Phi)$.

Proof. From Definition 2, the conditional PAoI can be written as

$$A_k = \hat{T}_{k-1} + Y_k = \hat{T}_{k-1} + V_k + T_k.$$

Since $\hat{T}_{k-1}$, V_k, and T_k are independent of each other and also themselves across k, the `mgf` of A_k for a given Φ becomes

$$\mathcal{M}_{A_k}(t) = \mathcal{M}_{\hat{T}_k}(t)\mathcal{M}_{A_k}(t)\mathcal{M}_{T_k}(t).$$

We have $\hat{T}_k \sim \texttt{Geo}(q_\mathrm{s})$ for $\hat{T}_k \geq 1$ (from Lemma 2), $V_k \sim \texttt{Geo}(\lambda_a)$ for $V_k \geq 0$ (from (8)), and $T_k \sim \texttt{Geo}(\xi\mu_\Phi)$ for $T_k \geq 1$ (from (7)). Therefore, (27) follows by substituting the `mgf`s of geometric distributions with above parameters. Next, (28) directly follows by substituting the means of $\hat{T}_k$, V_k, and T_k in A_k. □

Remark 2. *From* (9) *and* (28)*, it is evident that the conditional mean PAoI observed by the typical SD link with a preemptive queue is strictly less than that with a non-preemptive queue for any λ_a as long as $\xi\mu_\Phi < 1$. From* (9) *and* (28)*, we can verify that*

$$\lim_{\lambda_\mathrm{a}\to 1} \bar{A}_\mathrm{NP}(\beta;\Phi) = \frac{2}{\xi\mu_\Phi} \quad \textit{and} \quad \lim_{\lambda_\mathrm{a}\to 1} \bar{A}_\mathrm{P}(\beta;\Phi) = 1 + \frac{1}{\xi\mu_\Phi}.$$

From this, we can say that preemptive discipline reduces the mean PAoI almost by a factor of two compared to the non-preemptive discipline in the asymptotic regime of λ_a when $\xi\mu_\Phi$ is low. Further, we can also verify that

$$\lim_{\xi\mu_\Phi\to 1} \bar{A}_\mathrm{NP}(\beta;\Phi) = \lim_{\xi\mu_\Phi\to 1} \bar{A}_\mathrm{P}(\beta;\Phi) = \mathcal{Z}_\mathrm{a} + 2.$$

This implies that the sources observing high successful transmission probability can select any one of these queueing disciplines without much compromising on the mean PAoI when $\xi = 1$. Besides, note that this performance analysis also holds for the case where the sources can selectively opt for any one of these queueing disciplines. This is essentially because of the same transmission activities for any given source under both of these queues, as will discussed next.

B. Activity and Distribution of μ_Φ

As the preemptive queue just replaces the older updates with the newly arriving updates during the retransmission instances, its transmission rate is the same as that of the non-preemptive queue. In fact, the state diagrams for both these queue disciplines are equivalent (please refer to Fig. 3). As a result, the conditional steady state distributions (and thus the conditional activities), for a given μ_Φ, are also the same for both of these queues and are given by (11).

The point process of interferers is characterized by their activities, which is the same for both queue disciplines. As a result, the distributions of the conditional success probability μ_Φ must also be the same for both of these queues. Based on these arguments, the moments and approximate distribution of the conditional success probability μ_Φ presented in Lemma 1 along with the distribution of transmission activities of interfering sources given in (15) can be directly extended for the analysis of AoI under preemptive queue.

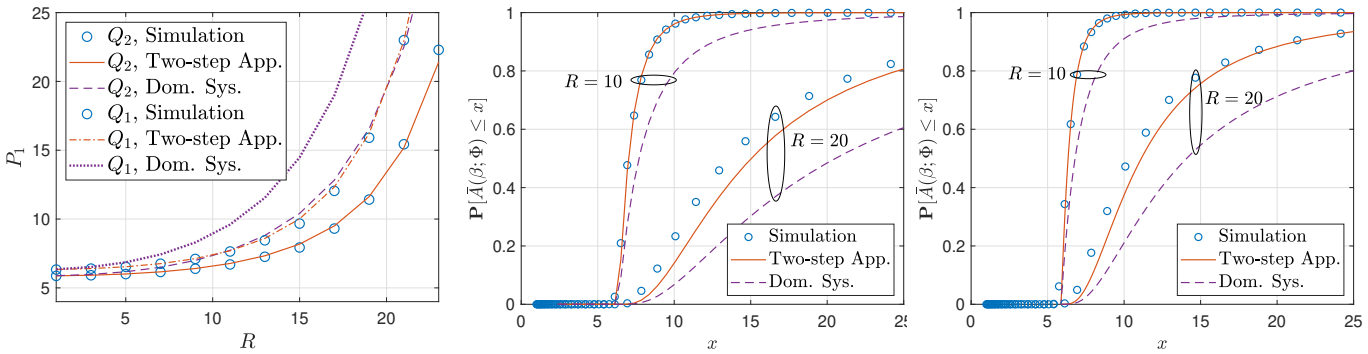

Figure 7. Verification of the proposed analytical framework: Average of the conditional mean PAoI (Left) and the spatial distribution of the conditional mean PAoI for non-preemptive (Middle) and preemptive (Right) disciplines.

C. Moments and Distribution of $\bar{A}_{\mathrm{P}}(\beta;\Phi)$

In this subsection, we derive bounds on the b-th moment and the distribution of $\bar{A}_{\mathrm{P}}(\beta;\Phi)$ using the two-step analysis of conditional success probability presented in Section III-D.

Theorem 3. *The upper bound of the b-th moment of the conditional mean PAoI for preemptive queueing discipline with no storage is*

$$P_b = \sum_{l+m+n=b} \binom{b}{l,m,n} \mathcal{Z}_{\mathrm{a}}^{l} \xi^{-m} S(n;m), \tag{29}$$

where $\binom{b}{l,m,n} = \frac{b!}{l!m!n!}$, $S(n;m) =$

$$\sum_{k=0}^{\infty} \binom{n+k-1}{k} (1-\lambda_{\mathrm{a}})^{k} \sum_{l=0}^{k} (-1)^{l} \binom{k}{l} \xi^{l} M_{l-m}, \tag{30}$$

and M_l is evaluated using Lemma 1 by setting $\bar{p}_m = \bar{p}_m^{\mathrm{D}}$ which is given in (16).

Proof. Please refer to Appendix D for the proof. □

The general result presented above can be used to derive simple expressions for the first two moments of $\bar{A}_2(\beta;\Phi)$, which are presented next.

Corollary 3. *The upper bound of the first two moments of the conditional mean PAoI for preemptive queueing discipline with no storage are*

$$P_1 = \mathcal{Z}_a + \xi_{-1} M_{-1} + S(1;0), \tag{31}$$

$$P_2 = \mathcal{Z}_a^2 + 2\mathcal{Z}_a \xi^{-1} M_{-1} + \xi^{-2} M_{-2} + 2\mathcal{Z}_{\mathrm{a}} S(1;0) + 2\xi^{-1} S(1;1) + S(2;0), \tag{32}$$

where $S(n;m)$ is given in (30) *and*

$$M_l = \exp\left(-\pi \lambda_{sd} \beta^{\delta} R^2 \hat{\delta} C_{\zeta_o}(l)\right),$$

such that

$$C_{\zeta_o}(l) = \sum_{m=1}^{l} \binom{l}{m} \binom{\delta-1}{m-1} \bar{p}_m^{\mathrm{D}},$$

for $l \geq 0$ and $C_{\zeta_o}(l)$ for $l = -1$ and $l = -2$ is given in (22) *and* (23)*, The distribution of ζ_o is given in* (15) *and $\bar{p}_m^{\mathrm{D}}$ is given in* (16)*.*

Proof. Please refer to Appendix E for the proof. □

The following corollary presents an approximate distribution of $\bar{A}_{\mathrm{P}}(\beta;\Phi)$.

Corollary 4. *Under the beta approximation, the* CDF *of the conditional mean PAoI for preemptive queueing discipline queue is*

$$F(x;\beta) = B_{g_{\mu_\Phi}(x)}(\kappa_1, \kappa_2) \tag{33}$$

where $g_{\mu_\Phi}(x) = \left\{\mu_\Phi \in [0,1] : \bar{A}_2(\beta;\Phi) = x\right\}$, and κ_1 and κ_2 are obtain using Lemma 1 by setting $\bar{p}_m = \bar{p}_m^{\mathrm{D}}$.

Proof. Let $g_{\mu_\Phi} = \bar{A}_2(\beta;\Phi)$ is a function of μ_Φ. Therefore, the CDF of $\bar{A}_2(\beta;\Phi)$ becomes

$$\mathbb{P}[\bar{A}_{\mathrm{P}}(\beta;\Phi) \leq x] = \mathbb{P}[\mu_\Phi \leq g_{\mu_\Phi}(x)] = 1 - \mathrm{D}(g_{\mu_\Phi}(x)),$$

where $g_{\mu_\Phi}(x) = \left\{\mu_\Phi \in [0,1] : \bar{A}_2(\beta;\Phi) = x\right\}$. Next, using the beta approximation for the distribution of μ_Φ given in Lemma 1, we obtain (33). The parameters κ_1 and κ_2 of the beta approximation are obtained using the two-step analysis by setting $\bar{p}_m = \bar{p}_m^{\mathrm{D}}$ in (14). □

V. Numerical Results and Discussion

This paper presents a new approach of the two-step system level modification for enabling the success probability analysis when the queues at the SD pairs are correlated. Therefore, before presenting the numerical analysis of the PAoI, we verify the application of this new two-step analytical framework for characterizing the PAoI using simulation results in the following subsection. Throughout this section, we consider the system parameter as $\lambda_a = 0.3$ updates/slot, $\lambda_{\mathrm{sd}} = 10^{-3}$ links/m^2, $\xi = 0.5$, $R = 15$ m, $\beta = 3$ dB, and $\alpha = 4$ unless mentioned otherwise. In the figures, Q_1 and Q_2 indicate the curves correspond to the non-preemptive and preemptive queiueing disciplines, respectively.

Fig. 7 verifies the proposed two-step approach based analytical framework using the simulation results for different values of link distances R. Note that $R \in [10, 20]$ is a wide enough range when $\lambda_{\mathrm{sd}} = 10^{-3}$ links/m^2 (for which the dominant interfering source lies at an average distance of around 15 m). Fig. 7 (Left) shows the spatial average of the conditional mean PAoI for both queuing disciplines, whereas Fig. 7 (Middle) and (Right) show the spatial distribution of the conditional mean PAoI for the non-preemptive (obtained using Cor. 2) and preemptive (obtained using Cor. 4) disciplines, respectively. From these figures, it is quite apparent that the proposed two-step approach provides significantly tighter bounds as compared to the conventional dominant system

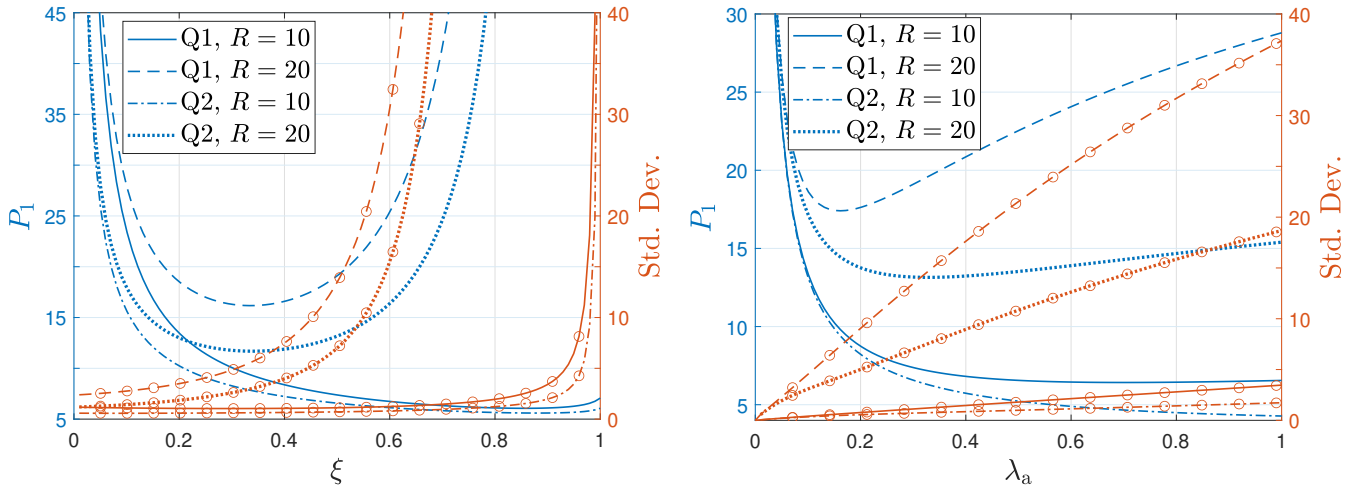

Figure 9. Mean and SD of $\bar{A}(\beta;\Phi)$ with respect to medium access probability ξ. The plane curves correspond to the mean, whereas the circular marked curves correspond to Std. Dev.

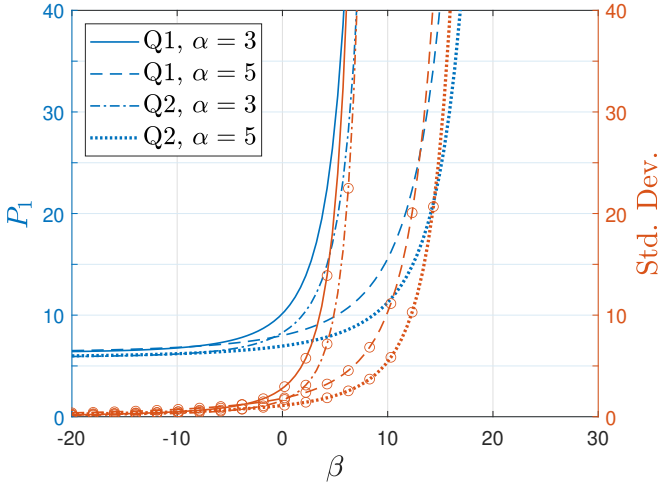

Figure 8. Mean and SD of $\bar{A}(\beta;\Phi)$ with respect to SIR threshold β for $R = 10$. The plane curves correspond to the mean, whereas the circular marked curves correspond to Std. Dev.

based approaches. The spatial distribution (for larger R) is somewhat loose as compared to the spatial average. This is because an additional approximation (beta approximation) is used to obtain the distribution of $\bar{A}(\beta;\Phi)$.

The performance trends of the conditional mean PAoI $\bar{A}(\beta;\Phi)$ with respect to the SIR threshold β and the path-loss exponent α are presented in Fig. 8. It may be noted that the success probability decreases with the increase in β and decrease in α. As a result, we can observe from Fig. 8 that the mean of $\bar{A}(\beta;\Phi)$, i.e., P_1, also degrades with respect to these parameters in the same order (under both types of queues). As expected, it is also observed that P_1 increases sharply around the value of β where the success probability approaches zero. On the other hand, P_1 converges to a constant value as β approaches zero where the success probability is almost one. In this region, P_1 only depends on the packet arrival rate λ_a and medium access probability ξ. For $\lambda_a = 0.3$ and $\xi = 0.5$, we can obtain $P_1 \approx 6.33$ for non-preemptive queue and $P_1 \approx 5.56$ for preemptive queue by plugging $\mu_\Phi = 1$ in (9) and (28), respectively. These values of P_1 can be verified from Fig. 8 when $\beta \leq 0$.

Further, it can be observed from Fig. 8 that the standard deviations of $\bar{A}(\beta;\Phi)$ follow a similar trend as that of P_1 except at $\beta \to 0$. This implies that the second moment of $\bar{A}(\beta;\Phi)$, i.e., P_2, increases at a faster rate than the one of P_1^2 with respect to β and α. In fact, this trend of P_1 and P_2 also holds for the other systems parameters which we discuss next.

Now, we present the performance trends of the mean and standard deviation of the conditional mean PAoI with respect to the medium access probability ξ and the status update arrival rate λ_a in Fig. 9 (left) and Fig. 9 (right), respectively. From these results, it can be seen that P_1 approaches to infinity as λ_a and/or ξ drop to zero. This is because the expected inter-arrival times between updates approach infinity as $\lambda_a \to 0$ and the expected delivery time approaches infinity as $\xi \to 0$. On the contrary, increasing λ_a and ξ reduces the inter-arrival and delivery times of the status updates which reduces P_1. However, P_1 again increases with further increase in λ_a and ξ. This is because the activities of the interfering SD pairs increase significantly at higher values of λ_a and ξ, which causes severe interference and hence increases P_1. However, its rate of increase depends upon the success probability, which further depends upon the wireless link parameters such as the link distance R, SIR threshold β, path-loss exponent α. For example, the figure shows that P_1 increases at a faster rate with λ_a and ξ when R is higher.

Fig. 10 (Left) shows an interesting fact that the same level of mean PAoI performance (below a certain threshold) can be achieved across the different densities of SD pairs λ_{sd} just by controlling the medium access probability ξ. The figure shows that higher ξ is a preferable choice for the lightly dense network (i.e., smaller λ_{sd}). This is because the tolerable interference in slightly dense scenario allows to choose higher ξ without affecting success probability which in turn provides to the better service rate. On the hand, smaller ξ is a preferable choice for highly dense network (i.e., larger

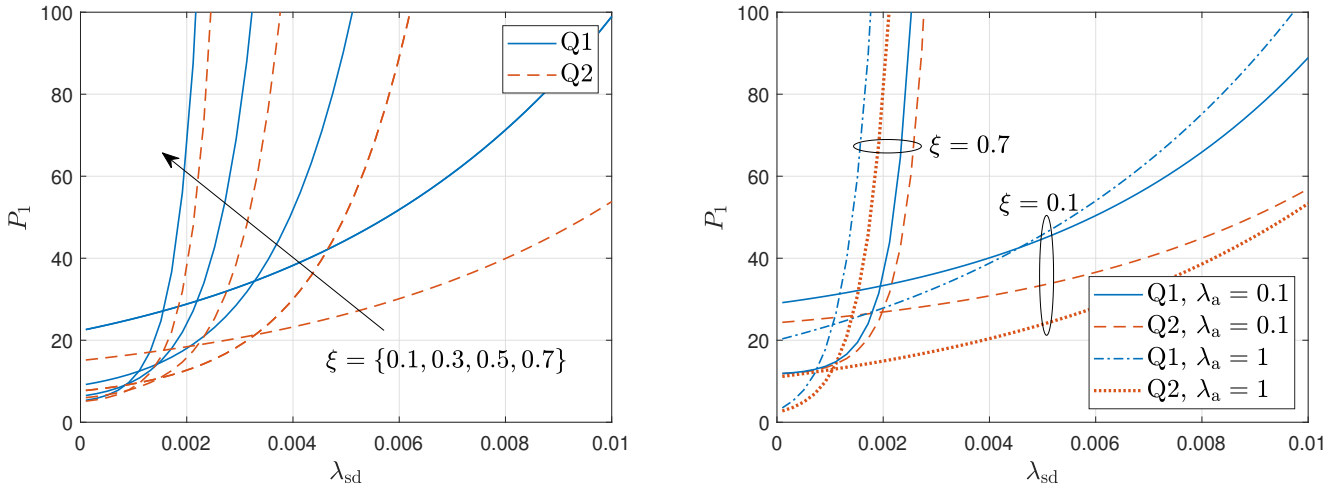

Figure 10. Mean of $\bar{A}(\beta;\Phi)$ with respect to the density of SD pairs $\lambda_{\rm a}$.

$\lambda_{\rm sd}$). This is because the smaller ξ can help to manage the severe interference in dense scenario, which in turn gives the better service rate.

In addition, Fig. 10 (Right) shows that ξ allows to manage the mean PAoI performance more efficiently as compared to the update arrival rate $\lambda_{\rm a}$ for different network densities. Furthermore, from the curves corresponding to Q_1 for $\xi = 0.1$ in Fig. 10 (Right), it is interesting to note that lowering $\lambda_{\rm a}$ with the increase of $\lambda_{\rm sd}$ allows to achieve better mean PAoI performance. This follows since the smaller $\lambda_{\rm a}$ aids to reduce the activities of sources, which is beneficial to alleviate interference and thus provide better service rate in the dense scenario.

VI. Conclusion

This paper considered a large-scale wireless network consisting of SD pairs whose locations follow a bipolar PPP. The source nodes are supposed to keep the information status at their corresponding destination nodes fresh by sending status updates over time. The PAoI metric was used to measure the freshness of information at the destination nodes. For this system setup, we developed a novel stochastic geometry-based approach that allowed us to derive a tight upper bound on the spatial moments of the conditional mean PAoI with no storage facility under preemptive and non-preemptive queue disciplines. The non-preemptive queue drops the newly arriving updates until the update in service is successfully delivered, whereas the preemptive queue discards the older update in service (or, retransmission) upon the arrival of a new update.

Our analysis provides several useful design insights. For instance, the analytical results demonstrate the impact of the update arrival rate, medium access probability and wireless link parameters on the spatial mean and variance of the conditional mean PAoI. The key observation was that preemptive queue reduces the mean PAoI almost by a factor two compared to the non-preemptive queue in the asymptotic regime of the update arrival rate when the success probability is relatively smaller. Our numerical results also reveal that the medium access probability plays an important role as compared to the update arrival rate for ensuring better mean PAoI performance under different network densities.

As a promising avenue of future work, one can analyze AoI for a system wherein the destinations are collecting status updates from multiple sources in their vicinity regarding a common physical random process.

Appendix

A. Proof of Lemma 1

The b-th moment of the conditional successful probability μ_Φ given in (2) is

$$M_b = \mathbb{E}_{\Phi,p_{\mathbf{x}}}\left[\prod_{\mathbf{x}\in\Phi}\left(1-\frac{p_{\mathbf{x}}}{1+\beta^{-1}R^{-\alpha}\|\mathbf{x}\|^{\alpha}}\right)^b\right],$$
$$= \mathbb{E}_{\Phi}\left[\prod_{\mathbf{x}\in\Phi}\mathbb{E}_{p_{\mathbf{x}}}\left(1-\frac{p_{\mathbf{x}}}{1+\beta^{-1}R^{-\alpha}\|\mathbf{x}\|^{\alpha}}\right)^b\right],$$

where the second equality follows from the assumption of independent activity $p_{\mathbf{x}}$ for $\forall \mathbf{x}\in\Phi$. Now, using the binomial expansion $(1-x)^b = \sum_{m=0}^{\infty}(-1)^m\binom{b}{m}x^m$ for a general $b\in\mathbb{Z}$, we can write M_b

$$= \mathbb{E}_{\Phi}\left[\prod_{\mathbf{x}\in\Phi}\sum_{m=0}^{b}(-1)^m\binom{b}{m}\frac{\bar{p}_m}{(1+\beta^{-1}R^{-\alpha}\|\mathbf{x}\|^{\alpha})^m}\right],$$

where $\bar{p}_m = \mathbb{E}[p_{\mathbf{x}}^m]$ is the m-th moment of the activity. Further, applying the probability generating functional (PGFL) of homogeneous PPP Φ, we obtain $M_b =$

$$\exp\left(-2\pi\lambda_{\rm sd}\int_0^{\infty}\left[1-\sum_{m=0}^{\infty}\binom{b}{m}\frac{(-1)^m\bar{p}_m}{\left(1+\frac{r^{\alpha}}{\beta R^{\alpha}}\right)^m}\right]r{\rm d}r\right),$$
$$= \exp\left(-2\pi\lambda_{\rm sd}\sum_{m=1}^{\infty}(-1)^{m+1}\binom{b}{m}\bar{p}_m\mathcal{W}_m(\beta,R)\right), \quad (34)$$

where

$$\mathcal{W}_m(\beta,R) = \int_0^{\infty}\frac{(\beta R^{\alpha})^m}{(\beta R^{\alpha}+r^{\alpha})^m}r{\rm d}r.$$

Using [42, Appendix A], $\mathcal{W}_m(\beta, R)$ can be evaluated as

$$\mathcal{W}_m(\beta,R) = \frac{1}{\alpha}(\beta R^\alpha)^m \int_0^\infty \frac{t^{1-\delta}}{(\beta R^\alpha + t)^m}\mathrm{d}t,$$
$$= (-1)^{m+1}\frac{\beta^\delta R^2}{\alpha}\binom{\delta-1}{m-1}\frac{\pi}{\sin(\delta\pi)}.$$

Finally, substituting the above solution in (34), we get (12).

B. Proof of Corollary 1

Solving (18) for $b = \{1, 2\}$ and then substituting M_{-1} and M_{-2} from Lemma 1, we obtain (19)-(21). From the definition of $C_{\zeta_o}(b)$, we can directly determine

$$C_{\zeta_o}(-1) = \mathbb{E}\Big[\sum_{m=1}^{\infty}\binom{-1}{m}\binom{\delta-1}{m-1}\zeta_o^m\Big],$$
$$= -\mathbb{E}\left[\zeta_o(1-\zeta_o)^{\delta-1}\right].$$

Now, for $b = -2$, let $C_{\zeta_o}(-2) = \mathbb{E}[B(\zeta_o, -2)]$ where

$$B(\zeta_o,-2) = \sum_{m=1}^{\infty}\binom{-2}{m}\binom{\delta-1}{m-1}\zeta_o^m,$$
$$= \sum_{m=1}^{\infty}(-1)^{2m-1}(m+1)\binom{m-1-\delta}{m-1}\zeta_o^m,$$
$$= -\sum_{m=1}^{\infty}\frac{(m-\delta)\Gamma(m-\delta)}{\Gamma(1-\delta)\Gamma(m)}\zeta_o^m + (\delta+1)\binom{m-1-\delta}{m-1}\zeta_o^m,$$
$$= -\sum_{m=1}^{\infty}\frac{\Gamma(2-\delta)}{\Gamma(2-\delta)}\frac{\Gamma(m-\delta+1)}{\Gamma(1-\delta)\Gamma(m)}\zeta_o^m + (\delta+1)\binom{m-1-\delta}{m-1}\zeta_o^m,$$
$$= -\sum_{m=1}^{\infty}\frac{\Gamma(2-\delta)}{\Gamma(1-\delta)}\binom{m-\delta}{m-1}\zeta_o^m + (\delta+1)\binom{m-1-\delta}{m-1}\zeta_o^m,$$
$$= -(1-\delta)\sum_{m=1}^{\infty}\binom{m-\delta}{m-1}\zeta_o^m - (\delta+1)\sum_{m=1}^{\infty}\binom{m-1-\delta}{m-1}\zeta_o^m,$$
$$= (\delta-1)\zeta_o\sum_{l=0}^{\infty}\binom{l+1-\delta}{l}\zeta_o^l - (\delta+1)\zeta_o\sum_{l=0}^{\infty}\binom{l-\delta}{l}\zeta_o^l$$
$$= (\delta-1)\zeta_o(1-\zeta_o)^{\delta-2} - (\delta+1)\zeta_o(1-\zeta_o)^{\delta-1}.$$

Finally, taking expectation of $B(\zeta_o, -2)$ with respect to ζ_o provides $C_{\zeta_o}(-2)$.

C. Proof of Lemma 2

Since the arrival process is Bernoulli, inter-arrival times τ_ns between updates are i.i.d. and also follow geometric distribution with parameter λ_a. From the fact that the sum of independent geometric random variables follows negative binomial distribution, we know

$$\mathbb{P}[X_n = K] = \binom{K-1}{n-1}\lambda_\mathrm{a}^n(1-\lambda_\mathrm{a})^{K-n}.$$

Now, we derive the distribution of $\hat{T}_k$ using the above pmfs of T_k and X_{N_k}. We start by first deriving the probabilities for the boundary values of $\hat{T}_k$ for given T_k. Since at least one slot is required for the successful update delivery, we have $1 \le \hat{T}_k \le T_k$. From Fig. 6, it can be observed that $\hat{T}_k = 1$ either if $T_k = 1$ or if there is a new arrival in the $(t_k + T_k)$-th time slot. Therefore, we can write

$$\mathbb{P}[\hat{T}_k = 1] = \mathbb{P}[T_k = 1] +$$
$$\times\, \mathbb{P}[\text{New Arrival Occurs in the } (t_k+T_k)\text{-th slot}]$$
$$= \xi\mu_\Phi + \lambda_\mathrm{a}(1-\xi\mu_\Phi). \tag{35}$$

It is worth noting that $\mathbb{P}[\hat{T}_k = 1]$ is independent of T_k. The other boundary case, i.e., $\hat{T}_k = T_k$, is possible only if there is no new update arrival in $[t_k, t'_k)$. Thus, we have

$$\mathbb{P}[\hat{T}_k = T_k] = (1-\lambda_\mathrm{a})^{T_k-1}. \tag{36}$$

Now, we determine the probability of $\hat{T}_k = m$ for $m \in \{2, \ldots, T_k - 1\}$. For $\hat{T}_k = m$, the following two conditions must hold so that we get $X_{N_k} = T_k - m$,

- the number of new arrivals within T_k are $N_k \in \{1, \ldots, T_k - m\}$, and
- there should not be a new arrival in $[t'_k - m, t'_k]$.

Therefore, for a given $T_k = s$, we have

$$\mathbb{P}[\hat{T}_k = m | T_k = s] = \mathbb{P}[\text{no arrival in } [t'_k - m, t'_k)]$$
$$\times\, \mathbb{P}[N_k = n \text{ such that } X_n = s - m],$$
$$= (1-\lambda_\mathrm{a})^m \sum_{n=1}^{s+1-m}\mathbb{P}[X_n = s-m],$$
$$= (1-\lambda_\mathrm{a})^m \sum_{n=1}^{s+1-m}\binom{s-m}{n-1}\lambda_\mathrm{a}^n(1-\lambda_\mathrm{a})^{s-m-n}. \tag{37}$$

For $T_k = s > 1$, from (35)-(37), we get $\mathbb{P}[\hat{T}_k = m | T_k = s]$

$$= \begin{cases} \lambda_\mathrm{a}, & \text{for } m = 1, \\ \sum_{n=1}^{s+1-m}\binom{s-m}{n-1}\lambda_\mathrm{a}^n(1-\lambda_\mathrm{a})^{s-n}, & \text{for } m = 2, \ldots, s-1, \\ (1-\lambda_\mathrm{a})^{m-1}, & \text{for } m = s. \end{cases} \tag{38}$$

Finally, we can determine the pmf of $\hat{T}_k$ for $m > 1$ as follows

$$\mathbb{P}[\hat{T}_k = m] = \sum_{s=m}^{\infty}\mathbb{P}[\hat{T}_k = m | T_k = s]\mathbb{P}[T_k = s],$$
$$= \mathbb{P}[\hat{T}_k = m | T_k = m]\mathbb{P}[T_k = m]$$
$$+ \sum_{s=m+1}^{\infty}\mathbb{P}[\hat{T}_k = m | T_k = s]\mathbb{P}[T_k = s],$$
$$= (1-\lambda_\mathrm{a})^{m-1}\xi\mu_\Phi(1-\xi\mu_\Phi)^{m-1}$$
$$+ \underbrace{\sum_{s=m+1}^{\infty}\xi\mu_\Phi(1-\xi\mu_\Phi)^{s-1}\sum_{n=1}^{s+1-m}\binom{s-m}{n-1}\lambda_\mathrm{a}^n(1-\lambda_\mathrm{a})^{s-n}}_{\mathcal{B}}.$$

where the last equality follows using (7) and (38). Substituting $s - m = l$ in the above term $\mathcal{B}$, we get

$$\mathcal{B} = \sum_{l=1}^{\infty}\xi\mu_\Phi(1-\xi\mu_\Phi)^{l+m-1}\sum_{n=1}^{l+1}\binom{l}{n-1}\lambda_\mathrm{a}^n(1-\lambda_\mathrm{a})^{l+m-n},$$
$$= \xi\mu_\Phi(1-\xi\mu_\Phi)^m(1-\lambda_\mathrm{a})^m\sum_{z=2}^{\infty}(1-\xi\mu_\Phi)^{z-2}$$
$$\times \sum_{n=1}^{z}\binom{z-1}{n-1}\lambda_\mathrm{a}^n(1-\lambda_\mathrm{a})^{z-1-n}.$$

Next, by substituting

$$\sum_{n=1}^{l}\binom{l-1}{n-1}\lambda_{\rm a}^{n}(1-\lambda_{\rm a})^{l-n}=\lambda_{\rm a},$$

and $z-2=a$, we obtain

$$\begin{aligned}\mathcal{B}&=\lambda_{\rm a}\xi\mu_\Phi(1-\xi\mu_\Phi)^m(1-\lambda_{\rm a})^{m-1}\sum_{a=0}^{\infty}(1-\xi\mu_\Phi)^a,\\&=\lambda_{\rm a}(1-\xi\mu_\Phi)^m(1-\lambda_{\rm a})^{m-1},\end{aligned}$$

where the last equality follows using the power series $\sum_{n=0}^{\infty}x^n=\frac{1}{1-x}$ for $|x|<1$. Finally, substituting $\mathcal{B}$ in $\mathbb{P}[\hat{T}_k=m]$, we get $\mathbb{P}[\hat{T}_k=m]=$

$$\begin{aligned}&\xi\mu_\Phi(1-\xi\mu_\Phi)^{m-1}(1-\lambda_{\rm a})^{m-1}+\lambda_{\rm a}(1-\xi\mu_\Phi)^m(1-\lambda_{\rm a})^{m-1},\\&=\left(\xi\mu_\Phi+\lambda_{\rm a}(1-\xi\mu_\Phi)\right)(1-\xi\mu_\Phi)^{m-1}(1-\lambda_{\rm a})^{m-1},\end{aligned}\tag{39}$$

for $m>1$. Therefore, using (35) and (39), we obtain (26).

D. Poof of Theorem 3

Let $\mathcal{S}_{\rm a}=\xi\mu_\Phi(1-\lambda_{\rm a})+\lambda_{\rm a}$ be the denominator of the last term in (28). Since $\lambda_{\rm a}\in(0,1)$, $\mathcal{S}_{\rm a}$ represents the convex combination of 1 and $\xi\mu_\Phi$. As $\xi\mu_\Phi\in(0,1)$, we have $0<\mathcal{S}_{\rm a}<1$. Therefore, using the following binomial expansion

$$(1+x)^{-n}=\sum_{k=0}^{\infty}(-1)^k\binom{n+k-1}{k}x^k\text{ for }|x|<1,$$

we can write

$$\mathcal{S}_{\rm a}^{-n}=(1+(\mathcal{S}_{\rm a}-1))^{-n}=\sum_{k=0}^{\infty}(-1)^k\binom{n+k-1}{k}(\mathcal{S}_{\rm a}-1)^k.$$

Note that $(\mathcal{S}_{\rm a}-1)^k=[\xi\mu_\Phi(1-\lambda_{\rm a})-(1-\lambda_{\rm a})]^k=(-1)^k(1-\lambda_{\rm a})^k(1-\xi\mu_\Phi)^k$. Using this, we can obtain the expectation of $\mu_\Phi^{-m}\mathcal{S}_{\rm a}^{-n}$ as

$$\begin{aligned}S(n;m)&=\mathbb{E}\left[\mu_\Phi^{-m}\mathcal{S}_{\rm a}^{-n}\right],\\&=\mathbb{E}\left[\mu_\Phi^{-m}\sum_{k=0}^{\infty}\binom{n+k-1}{k}(1-\lambda_{\rm a})^k(1-\xi\mu_\Phi)^k\right],\\&=\sum_{k=0}^{\infty}\binom{n+k-1}{k}(1-\lambda_{\rm a})^k\sum_{l=0}^{k}(-1)^l\binom{k}{l}\xi^lM_{l-m}.\end{aligned}$$

Using this and (28), we now derive the b-th moment of $\bar{A}_{\rm P}(\beta;\Phi)$ as

$$\begin{aligned}P_b&=\mathbb{E}\left[\left(\mathcal{Z}_{\rm a}+\frac{1}{\xi\mu_\Phi}+\frac{1}{\xi\mu_\Phi(1-\lambda_{\rm a})+\lambda_{\rm a}}\right)^b\right],\\&=\sum_{l+m+n=b}\binom{b}{l,m,n}\mathcal{Z}_{\rm a}^l\xi^{-m}\mathbb{E}\left[\mu_\Phi^{-m}\mathcal{S}_{\rm a}^{-n}\right].\end{aligned}$$

Further, substituting $\mathbb{E}\left[\mu_\Phi^{-m}\mathcal{S}_{\rm a}^{-n}\right]=S(n;m)$ in the above expression, we obtain (29). Since the moments of the upper bound of the activity probabilities of interfering sources (given in (16)) are used for evaluating the moments of μ_Φ, the resulting b-th moment of $\bar{A}_{\rm P}(\beta;\Phi)$ in (29) is in fact an upper bound.

E. Proof of Corollary 3

Using $\mathbb{E}\left[\mu_\Phi^{-m}\mathcal{S}_{\rm a}^{-n}\right]=S(n;m)$ and (28), the mean of $\bar{A}_{\rm P}(\beta;\Phi)$ can be determined as $P_1=$

$$\mathcal{Z}_{\rm a}+\xi^{-1}\mathbb{E}_\Phi\left[\mu_\Phi^{-1}\right]+\mathbb{E}_\Phi\left[\mathcal{S}_{\rm a}^{-1}\right]=\mathcal{Z}_{\rm a}+\xi^{-1}M_{-1}+S(1;0).$$

Similarly, the second moment of $\bar{A}_{\rm P}(\beta;\Phi)$ can be determined as

$$\begin{aligned}P_2&=\mathbb{E}\left[\left(\mathcal{Z}_{\rm a}+(\xi\mu_\Phi)^{-1}+\mathcal{S}_{\rm a}^{-1}\right)^2\right],\\&=\mathcal{Z}_{\rm a}^2+2\mathcal{Z}_{\rm a}\xi^{-1}M_{-1}+\xi^{-2}M_{-2}\\&\quad+2\mathcal{Z}_{\rm a}S(1;0)+2\xi^{-1}S(1;1)+S(2;0).\end{aligned}$$

Further, substitution of M_l from Lemma 1 provides the first two moments of $\bar{A}_{\rm P}(\beta;\mu_\Phi)$ as in (31) and (32). The values of $C_{\zeta_o}(l)$ for $l\in\{-1,-2\}$ directly follow from Corollary 1. However, the upper limit of the summation in $C_{\zeta_o}(l)$ for $l>0$ reduces to l (refer to Appendix A). Since the lower bounds of the moments of μ_Φ obtained from the two-step analysis are used here, the moments of $\bar{A}_{\rm P}(\beta;\Phi)$ given in (31) and (32) are the upper bounds (please refer to Section III-D for more details about the constructions and assumptions).

REFERENCES

[1] P. D. Mankar, M. A. Abd-Elmagid, and H. S. Dhillon, "Stochastic geometry-based analysis of the distribution of peak age of information," *IEEE Intl. Conf. Commun.*, 2021, (accepted).

[2] M. A. Abd-Elmagid, N. Pappas, and H. S. Dhillon, "On the role of age of information in the Internet of things," *IEEE Commun. Magazine*, vol. 57, no. 12, pp. 72–77, 2019.

[3] S. Kaul, R. Yates, and M. Gruteser, "Real-time status: How often should one update?" in *Proc., IEEE INFOCOM*, 2012.

[4] R. D. Yates and S. Kaul, "Real-time status updating: Multiple sources," in *IEEE Intl. Sym. Inf. Theory*, 2012.

[5] M. Costa, M. Codreanu, and A. Ephremides, "On the age of information in status update systems with packet management," *IEEE Trans. Inf. Theory*, vol. 62, no. 4, pp. 1897–1910, 2016.

[6] C. Kam, S. Kompella, and A. Ephremides, "Age of information under random updates," in *IEEE Intl. Sym. Inf. Theory*, 2013.

[7] L. Huang and E. Modiano, "Optimizing age-of-information in a multi-class queueing system," in *IEEE Intl. Sym. Inf. Theory*, 2015.

[8] K. Chen and L. Huang, "Age-of-information in the presence of error," in *IEEE Intl. Sym Inf. Theory*, 2016.

[9] B. Barakat, S. Keates, I. Wassell, and K. Arshad, "Is the zero-wait policy always optimum for information freshness (peak age) or throughput?" *IEEE Commun. Letters*, vol. 23, no. 6, pp. 987–990, June 2019.

[10] A. Kosta, N. Pappas, A. Ephremides, and V. Angelakis, "Age and value of information: Non-linear age case," in *IEEE Intl. Sym. Inf. Theory*, 2017.

[11] A. Javani and Z. Wang, "Age of information in multiple sensing of a single source," 2019, available online: arxiv.org/abs/1902.01975.

[12] Y. Inoue, H. Masuyama, T. Takine, and T. Tanaka, "A general formula for the stationary distribution of the age of information and its application to single-server queues," *IEEE Trans. Info. Theory*, vol. 65, no. 12, pp. 8305–8324, 2019.

[13] A. Kosta, N. Pappas, A. Ephremides, and V. Angelakis, "Non-linear age of information in a discrete time queue: Stationary distribution and average performance analysis," 2020, available online: arxiv.org/abs/2002.08798.

[14] J. P. Champati, H. Al-Zubaidy, and J. Gross, "On the distribution of aoi for the GI/GI/1/1 and GI/GI/1/2* systems: Exact expressions and bounds," in *Proc., IEEE INFOCOM*, 2019.

[15] O. Ayan, H. M. Gürsu, A. Papa, and W. Kellerer, "Probability analysis of age of information in multi-hop networks," *IEEE Netw. Lett.*, 2020.

[16] R. D. Yates, "The age of information in networks: Moments, distributions, and sampling," 2018, available online: arxiv.org/abs/1806.03487.

[17] I. Kadota, E. Uysal-Biyikoglu, R. Singh, and E. Modiano, "Minimizing the age of information in broadcast wireless networks," in *Proc., Allerton Conf. on Commun., Control, and Computing*, 2016.

[18] Y.-P. Hsu, E. Modiano, and L. Duan, "Scheduling algorithms for minimizing age of information in wireless broadcast networks with random arrivals," *IEEE Trans. on Mobile Computing*, to appear.

[19] M. Bastopcu and S. Ulukus, "Who should google scholar update more often?" in *Proc., IEEE INFOCOM Workshops*, 2020.

[20] B. Buyukates, A. Soysal, and S. Ulukus, "Age of information in Two-hop multicast networks," in *Proc., IEEE Asilomar*, 2018.

[21] J. Li, Y. Zhou, and H. Chen, "Age of information for multicast transmission with fixed and random deadlines in IoT systems," *IEEE Internet of Things Journal*, to appear.

[22] R. Talak, S. Karaman, and E. Modiano, "Minimizing age-of-information in multi-hop wireless networks," in *Proc., Allerton Conf. on Commun., Control, and Computing*, 2017.

[23] A. Arafa and S. Ulukus, "Timely updates in energy harvesting two-hop networks: Offline and online policies," *IEEE Trans. on Wireless Commun.*, vol. 18, no. 8, pp. 4017–4030, Aug. 2019.

[24] A. M. Bedewy, Y. Sun, and N. B. Shroff, "Optimizing data freshness, throughput, and delay in multi-server information-update systems," in *IEEE Intl. Sym. Inf. Theory*, 2016.

[25] Y. Gu, H. Chen, Y. Zhou, Y. Li, and B. Vucetic, "Timely status update in internet of things monitoring systems: An age-energy tradeoff," *IEEE Internet of Things Journal*, vol. 6, no. 3, pp. 5324–5335, 2019.

[26] M. A. Abd-Elmagid, H. S. Dhillon, and N. Pappas, "A reinforcement learning framework for optimizing age of information in RF-powered communication systems," *IEEE Trans. Commun.*. [Early Access].

[27] B. Zhou and W. Saad, "Joint status sampling and updating for minimizing age of information in the Internet of Things," *IEEE Trans. Commun.*, vol. 67, no. 11, pp. 7468–7482, 2019.

[28] M. A. Abd-Elmagid, H. S. Dhillon, and N. Pappas, "Online age-minimal sampling policy for RF-powered IoT networks," *Proc., IEEE Globecom*, Dec. 2019.

[29] G. Stamatakis, N. Pappas, and A. Traganitis, "Optimal policies for status update generation in an IoT device with heterogeneous traffic," *IEEE Internet of Things Journal*, 2020.

[30] M. A. Abd-Elmagid, H. S. Dhillon, and N. Pappas, "AoI-optimal joint sampling and updating for wireless powered communication systems," *IEEE Trans. Veh. Technol.*, 2020, [Early Access].

[31] B. Buyukates, A. Soysal, and S. Ulukus, "Age of information scaling in large networks," in *Proc., IEEE ICC*, 2019.

[32] B. Li, H. Chen, Y. Zhou, and Y. Li, "Age-oriented opportunistic relaying in cooperative status update systems with stochastic arrivals," 2020, available online: arxiv.org/abs/2001.04084.

[33] M. A. Abd-Elmagid and H. S. Dhillon, "Average peak age-of-information minimization in UAV-assisted IoT networks," *IEEE Trans. Veh. Technol.*, vol. 68, no. 2, pp. 2003–2008, Feb. 2019.

[34] M. A. Abd-Elmagid, A. Ferdowsi, H. S. Dhillon, and W. Saad, "Deep reinforcement learning for minimizing age-of-information in UAV-assisted networks," *Proc., IEEE Globecom*, Dec. 2019.

[35] M. K. Abdel-Aziz, C.-F. Liu, S. Samarakoon, M. Bennis, and W. Saad, "Ultra-reliable low-latency vehicular networks: Taming the age of information tail," in *Proc., IEEE Globecom*, 2018.

[36] M. Bastopcu and S. Ulukus, "Minimizing age of information with soft updates," *Journal of Commun. and Networks*, vol. 21, no. 3, pp. 233–243, 2019.

[37] E. Altman, R. El-Azouzi, D. S. Menasche, and Y. Xu, "Forever young: Aging control for hybrid networks," in *IEEE Intl. Sym. Mobile Ad Hoc Networking and Computing*, 2019.

[38] E. Hargreaves, D. S. Menasché, and G. Neglia, "How often should I access my online social networks?" in *IEEE MASCOTS*. IEEE, 2019.

[39] J. G. Andrews, F. Baccelli, and R. K. Ganti, "A tractable approach to coverage and rate in cellular networks," *IEEE Trans. on Commun.*, vol. 59, no. 11, pp. 3122–3134, Nov. 2011.

[40] H. S. Dhillon, R. K. Ganti, F. Baccelli, and J. G. Andrews, "Modeling and analysis of K-tier downlink heterogeneous cellular networks," *IEEE Journal on Sel. Areas in Commun.*, vol. 30, no. 3, pp. 550 – 560, Apr. 2012.

[41] F. Baccelli, B. Blaszczyszyn, and P. Muhlethaler, "An aloha protocol for multihop mobile wireless networks," *IEEE Trans. on Info. Theory*, vol. 52, no. 2, pp. 421–436, Feb 2006.

[42] M. Haenggi, "The meta distribution of the SIR in Poisson bipolar and cellular networks," *IEEE Trans. Wireless Commun.*, vol. 15, no. 4, pp. 2577–2589, 2016.

[43] S. S. Kalamkar and M. Haenggi, "Per-link reliability and rate control: Two facets of the sir meta distribution," *IEEE Wireless Commun. Lett.*, vol. 8, no. 4, pp. 1244–1247, 2019.

[44] Y. Zhong, T. Q. S. Quek, and X. Ge, "Heterogeneous cellular networks with spatio-temporal traffic: Delay analysis and scheduling," *IEEE JSAC*, vol. 35, no. 6, pp. 1373–1386, 2017.

[45] M. Emara, H. Elsawy, and G. Bauch, "A spatiotemporal model for peak AoI in uplink IoT networks: Time versus event-triggered traffic," *IEEE Internet Things J.*, vol. 7, no. 8, pp. 6762–6777, 2020.

[46] C. Saha, M. Afshang, and H. S. Dhillon, "Meta distribution of downlink sir in a Poisson cluster process-based HetNet model," *IEEE Wireless Communications Letters*, pp. 1–1, 2020.

[47] P. D. Mankar and H. S. Dhillon, "Downlink analysis of NOMA-enabled cellular networks with 3gpp-inspired user ranking," *IEEE Trans. Wireless Commun.*, vol. 19, no. 6, pp. 3796–3811, 2020.

[48] R. K. Ganti and M. Haenggi, "Spatial and temporal correlation of the interference in ALOHA ad hoc networks," *IEEE Commun. Lett.*, vol. 13, no. 9, pp. 631–633, 2009.

[49] R. R. Rao and A. Ephremides, "On the stability of interacting queues in a multiple-access system," *IEEE Trans. Inf. Theory*, vol. 34, no. 5, pp. 918–930, Sep. 1988.

[50] B. Bllaszczyszyn, R. Ibrahim, and M. K. Karray, "Spatial disparity of QoS metrics between base stations in wireless cellular networks," *IEEE Trans. on Commun.*, vol. 64, no. 10, pp. 4381–4393, Oct. 2016.

[51] M. Emara, H. El Sawy, and G. Bauch, "Prioritized multi-stream traffic in uplink iot networks: Spatially interacting vacation queues," *IEEE Internet Things J.*, 2020, [Early Access].

[52] G. Chisci, H. Elsawy, A. Conti, M. Alouini, and M. Z. Win, "Uncoordinated massive wireless networks: Spatiotemporal models and multiaccess strategies," *IEEE/ACM Trans. Netw.*, vol. 27, no. 3, pp. 918–931, 2019.

[53] H. Elsawy, "Characterizing IoT networks with asynchronous time-sensitive periodic traffic," *IEEE Wireless Commun. Lett.*, vol. 9, no. 10, pp. 1696–1700, 2020.

[54] H. H. Yang, T. Q. S. Quek, and H. V. Poor, "A unified framework for SINR analysis in Poisson networks with traffic dynamics," *IEEE Trans. Commun.*, [Early Access].

[55] H. H. Yang and T. Q. S. Quek, "Spatio-temporal analysis for SINR coverage in small cell networks," *IEEE Trans. Commun.*, vol. 67, no. 8, pp. 5520–5531, 2019.

[56] Y. Wang, H. H. Yang, Q. Zhu, and T. Q. S. Quek, "Analysis of packet throughput in spatiotemporal HetNets with scheduling and various traffic loads," *IEEE Wireless Commun. Lett.*, vol. 9, no. 1, pp. 95–98, 2020.

[57] H. H. Yang, A. Arafa, T. Q. S. Quek, and H. V. Poor, "Age of information in random access networks: A spatiotemporal study," 2020, available online: arxiv.org/abs/2008.07717.

[58] T. Bonald, S. Borst, N. Hegde, and A. Proutiére, *Wireless data performance in multi-cell scenarios*. ACM, 2004.

[59] Y. Zhong, M. Haenggi, T. Q. S. Quek, and W. Zhang, "On the stability of static Poisson networks under random access," *IEEE Trans. Commun.*, vol. 64, no. 7, pp. 2985–2998, July 2016.

[60] Y. Hu, Y. Zhong, and W. Zhang, "Age of information in Poisson networks," in *Proc., IEEE WCSP*, 2018.

[61] Y. Zhong, G. Mao, X. Ge, and F. c. Zheng, "Spatio-temporal modeling for massive and sporadic access," *IEEE Journal on Selected Areas in Communications*, 2020, [Early Access].

[62] H. H. Yang, A. Arafa, T. Q. Quek, and V. Poor, "Optimizing information freshness in wireless networks: A stochastic geometry approach," *IEEE Trans. Mobile Comput.*, [Early Access].

[63] P. D. Mankar, Z. Chen, M. A. Abd-Elmagid, N. Pappas, and H. S. Dhillon, "Throughput and age of information in a cellular-based IoT network," 2020, available online: arxiv.org/abs/2005.09547.

[64] M. Haenggi, *Stochastic geometry for wireless networks*. Cambridge University Press, 2012.

Praful D. Mankar (S'14–M'19) is an Assistant Professor at International Institute of Information Technology, Hyderabad, India. He received his B.E. degree in Electrical and Communication Engineering from Amravati University, MH, India, in 2006, and the M.Tech degree in telecommunications systems engineering and Ph.D. degree in wireless networks from IIT Kharagpur, WB, India, in 2009 and 2016, respectively. He also worked as a postdoctoral research associate in Wireless@VT research group at Virginia Tech, USA from 2017 to 2019. His research interests are primarily focused on the modeling and analysis of wireless networks using the application of stochastic geometry.

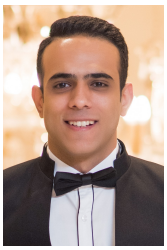

Mohamed A. Abd-Elmagid is a Ph.D. Candidate in the Bradley Department of Electrical and Computer Engineering at Virginia Tech. He received his B.Sc. degree in Electronics and Electrical Communications Engineering from Cairo University, Egypt in 2014 and M.S. degree in Wireless Communications from Nile University, Egypt in 2017. He worked as an Exchange Research Assistant at Sabanci University, Turkey, from Oct. 2016 to Feb. 2017. Prior to that, he was a Research Assistant at Nile University, Egypt, from Sep. 2014 to Sep. 2016. His research interests include cyber-physical internet of things systems, age of information, energy harvesting, wireless networks, machine learning, optimization and stochastic geometry.

Harpreet S. Dhillon (S'11–M'13–SM'19) received the B.Tech. degree in electronics and communication engineering from IIT Guwahati in 2008, the M.S. degree in electrical engineering from Virginia Tech in 2010, and the Ph.D. degree in electrical engineering from the University of Texas at Austin in 2013.

After serving as a Viterbi Postdoctoral Fellow at the University of Southern California for a year, he joined Virginia Tech in 2014, where he is currently an Associate Professor of electrical and computer engineering and the Elizabeth and James E. Turner Jr. '56 Faculty Fellow. His research interests include communication theory, wireless networks, stochastic geometry, and machine learning. He is a Clarivate Analytics Highly Cited Researcher and has coauthored five best paper award recipients including the 2014 IEEE Leonard G. Abraham Prize, the 2015 IEEE ComSoc Young Author Best Paper Award, and the 2016 IEEE Heinrich Hertz Award. He was named the 2017 Outstanding New Assistant Professor, the 2018 Steven O. Lane Junior Faculty Fellow, and the 2018 College of Engineering Faculty Fellow by Virginia Tech. His other academic honors include the 2008 Agilent Engineering and Technology Award, the UT Austin MCD Fellowship, and the 2013 UT Austin Wireless Networking and Communications Group leadership award. He currently serves as a Senior Editor for the IEEE WIRELESS COMMUNICATIONS LETTERS and an Editor for the IEEE TRANSACTIONS ON WIRELESS COMMUNICATIONS and the IEEE TRANSACTIONS ON GREEN COMMUNICATIONS AND NETWORKING.